

Supporting Information for

Thermal-Assisted Self-Assembly: A Self-Adaptive Strategy towards Large-Area Uniaxial Organic Single-Crystalline Microribbon Arrays

Yu Zhang,^a Xiaoting Zhu,^a Shuyuan Yang,^a Fei Zhai,^b Fei Zhang,^b Zhikai Niu,^a Yiyu Feng,^b Wei Feng,^b Xiaotao Zhang,^a liqiang Li,^c Rongjin Li^{*a} and Wenping Hu^a

^a Tianjin Key Laboratory of Molecular Optoelectronic Sciences, Department of Chemistry, School of Science, Tianjin University & Collaborative Innovation Center of Chemical Science and Engineering (Tianjin), Tianjin 300072, China.

E-mail: lirj@tju.edu.cn

^b School of Materials Science and Engineering, Tianjin University, Tianjin 300072, China

^c Institute of Molecular Aggregation Science, Tianjin University, Tianjin 300072, China

- (1) Figure S1. OM image of large-area TIPS-pentacene uniaxial OSCMAs.
- (2) Figure S2. OM image and histograms of the width of TIPS-pentacene uniaxial OSCMAs.
- (3) Figure S3. AFM image of an individual TIPS-PEN microribbon and height profile of the microribbon.
- (4) Figure S4. OM images of TIPS-pentacene crystals produced by drop-casting at different uniform temperature.
- (5) Figure S5. OM images of TIPS-pentacene crystals obtained on substrates tilting at different tilt angles without heating.
- (6) Figure S6. OM images of TIPS-pentacene crystals produced by the TASA method at different temperatures.
- (7) Figure S7. OM images of TIPS-pentacene crystals obtained from different concentrations.
- (8) Figure S8. Device performance of OFETs based on uniaxial OSCMAs of TIPS-pentacene.
- (9) Figure S9. Device performance of OFETs based on TIPS-pentacene films obtained by drop-casting on a hot plate.
- (10) Figure S10. UV-Vis of the TIPS-pentacene uniaxial OSCMAs.
- (11) Figure S11. POM images of the drop-casting TIPS-pentacene film.
- (12) Figure S12. OM images of Perylene and C8-BTBT grown by the TASA method.
- (13) Figure S13. OM images of TIPS-pentacene grown on glass, PET and quartz.
- (14) Figure S14. Typical OM images of TIPS-pentacene produced by the TASA method using chlorobenzene and mesitylene as the solvent.
- (15) Figure S15. OM images of TIPS-pentacene grown on OTS treated substrate.
- (16) Figure S16. Calculation of the channel width.
- (17) Table S1. Comparison of figure of merit of phototransistor based on organic semiconductors.

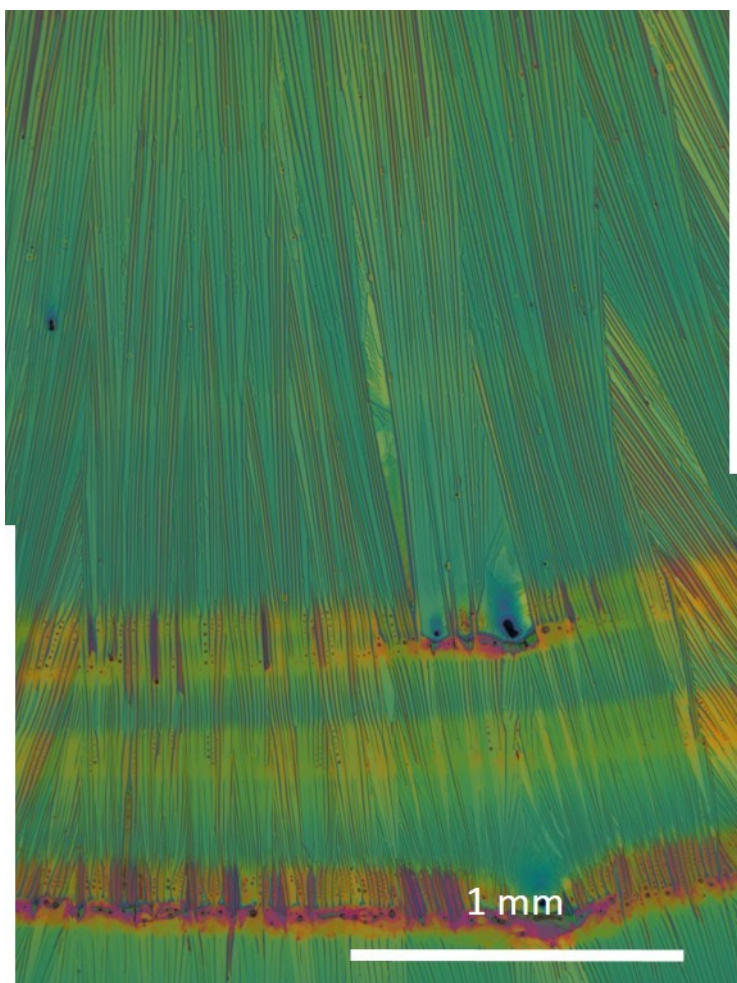


Figure S1. A coalesced optical microscope image of large-area TIPS-pentacene uniaxial OSCMA with millimeter-long ribbons.

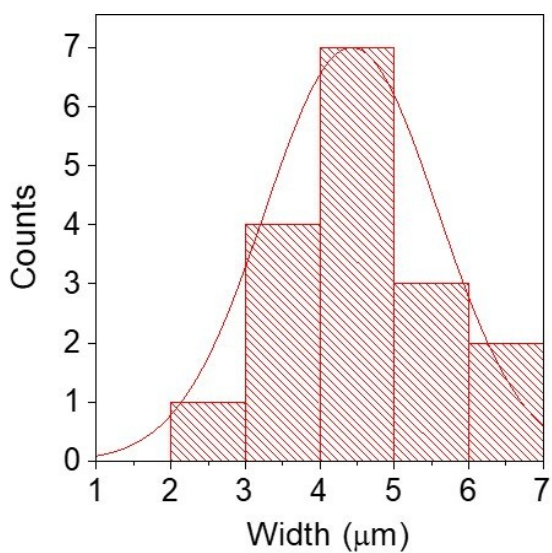
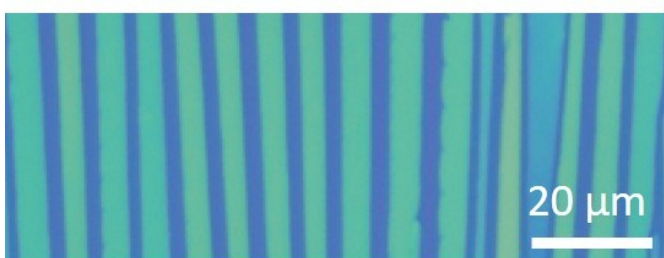


Figure S2. (a) Optical microscope image of TIPS-pentacene uniaxial OSCMA. (b) Histograms of the width of TIPS-pentacene uniaxial OSCMA.

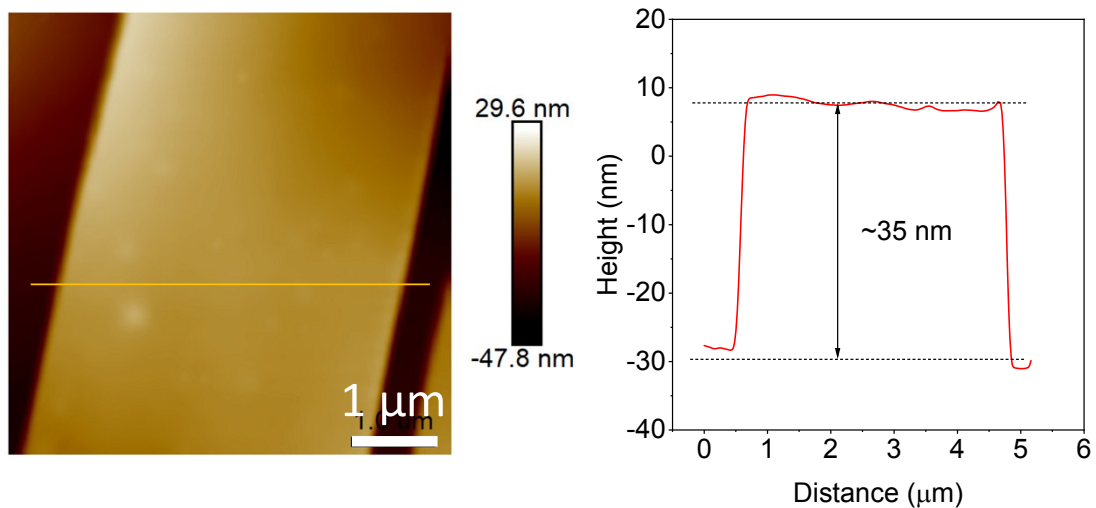


Figure S3. (a) AFM image of an individual TIPS-PEN microribbon. (b) Height profile of the microribbon.

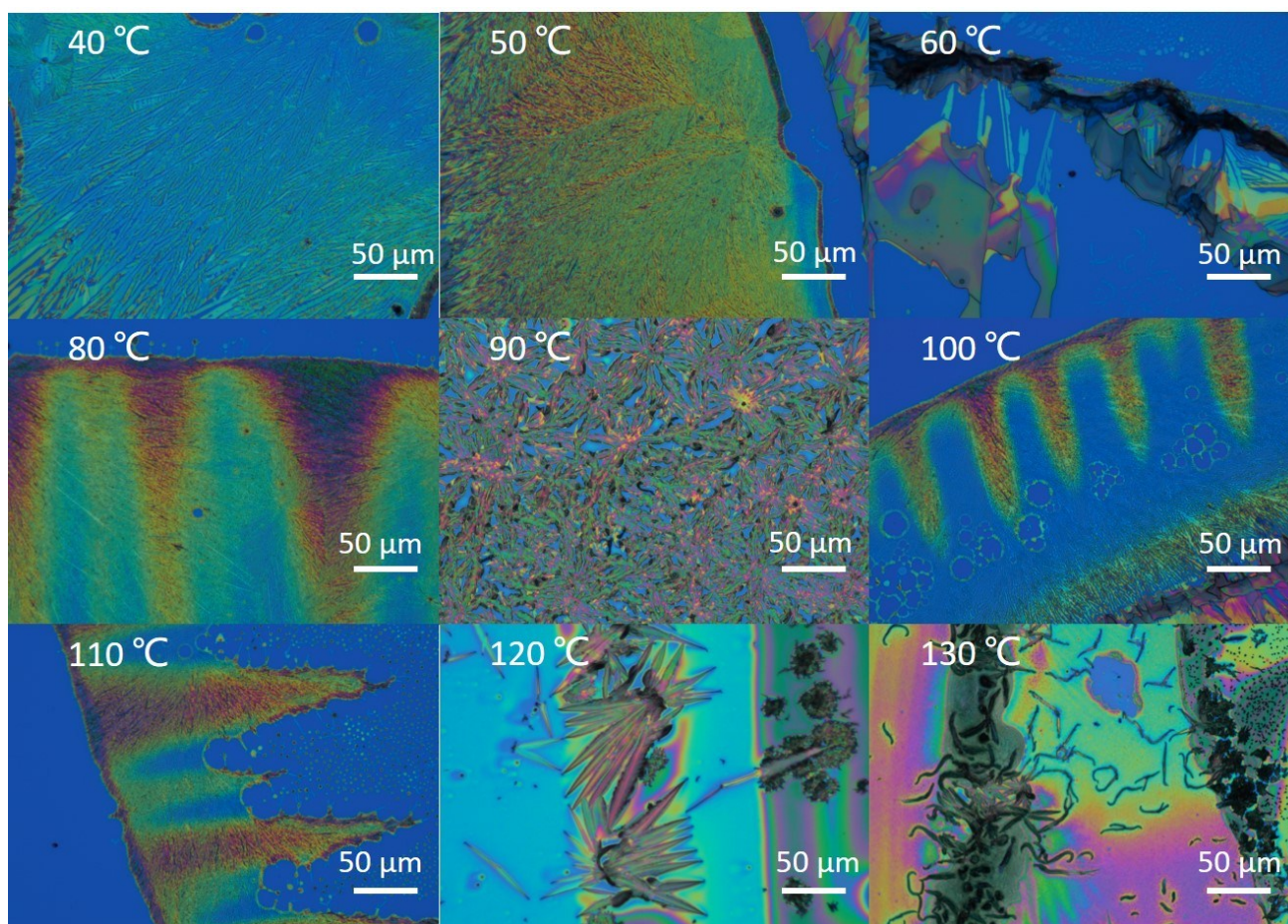


Figure S4. Optical microscope images of TIPS-pentacene crystals produced by drop-casting at different uniform temperature.

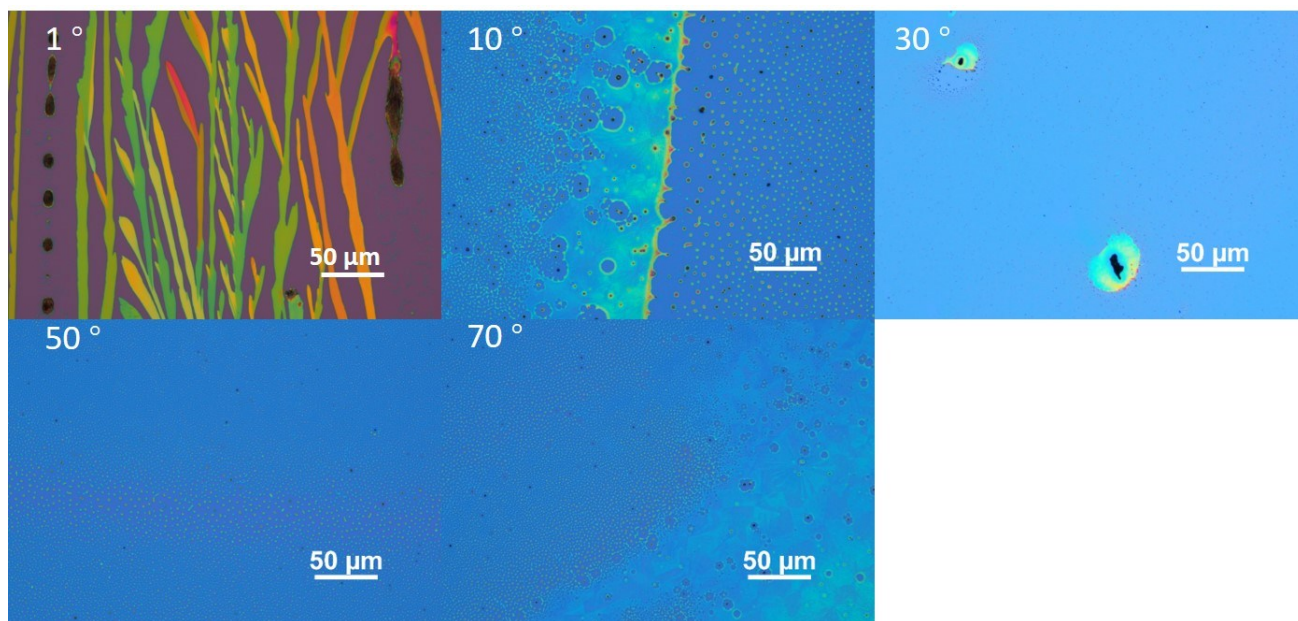


Figure S5. Optical microscope images of TIPS-pentacene crystals obtained on substrates tilting at different tilt angles without heating.

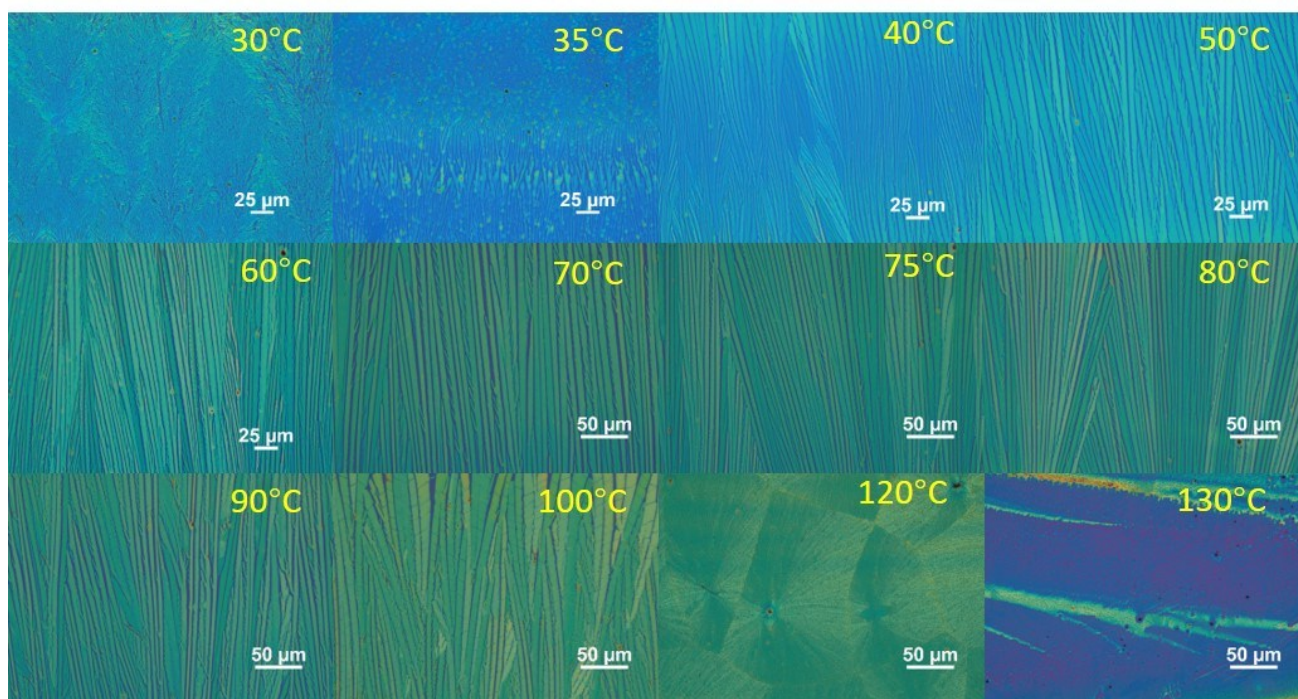


Figure S6. Optical microscope images of TIPS-pentacene crystals produced by the TASA method at different temperatures.

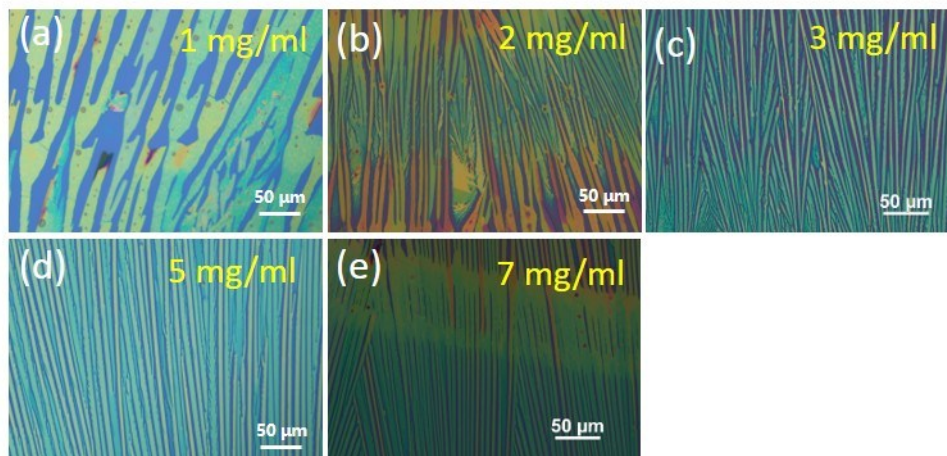


Figure S7. Optical microscope images of TIPS-pentacene crystals obtained from different concentrations.

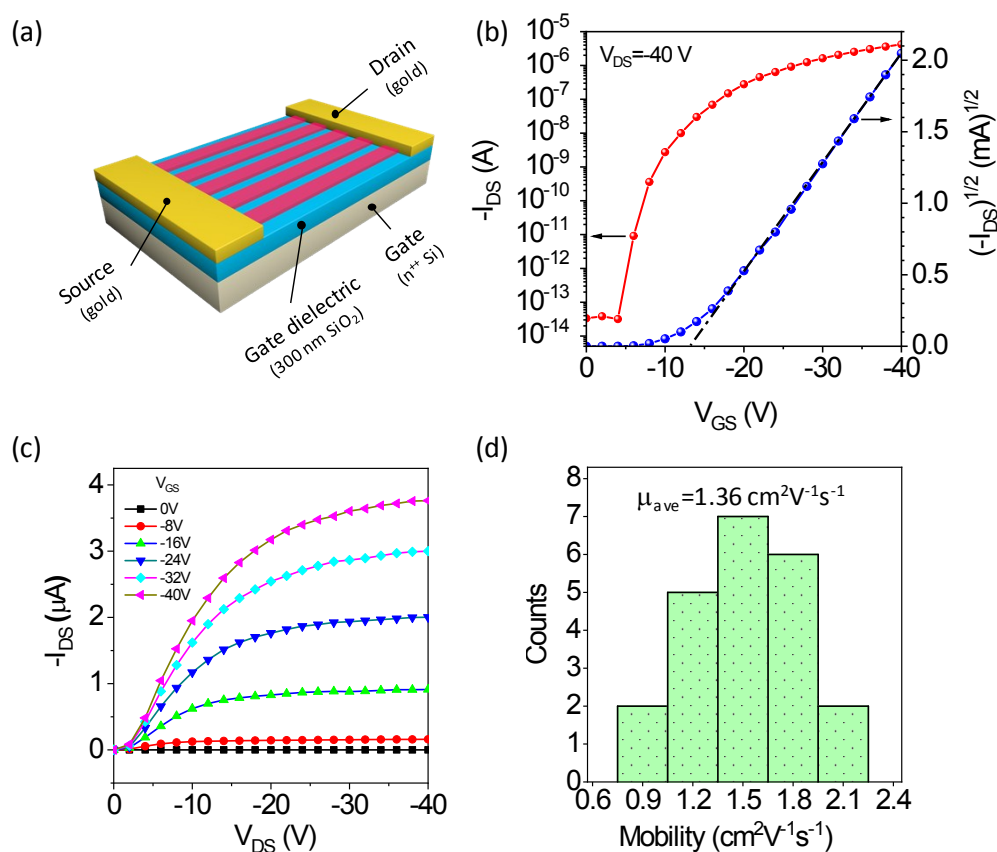


Figure S8. (a) Schematic of OFETs based on uniaxial OSCMAs of TIPS-pentacene. (b, c) The transfer and output curves of the OFETs. (d) Histogram of the hole mobilities calculated from 22 devices.

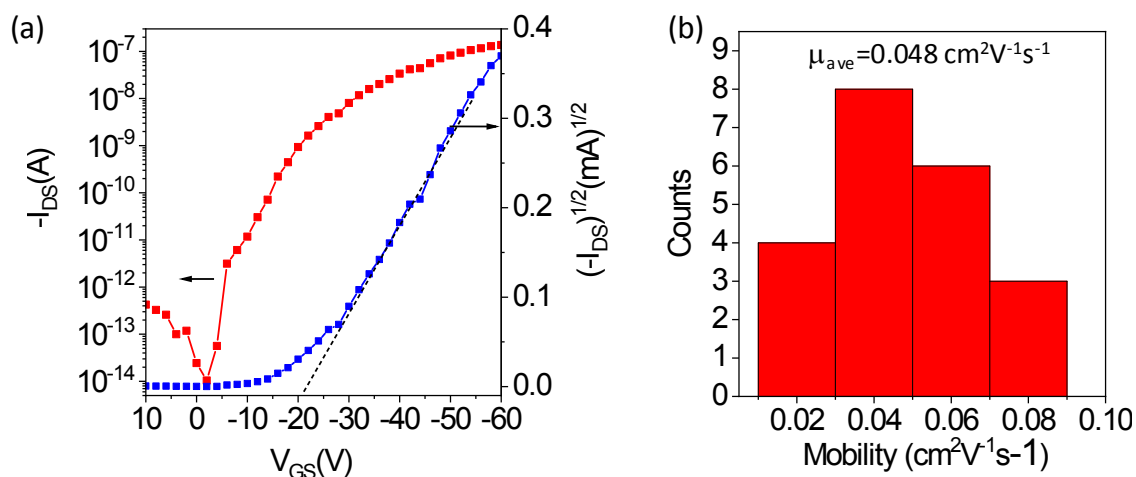


Figure S9. (a) Transfer characteristics of the OFETs based on TIPS-PEN films prepared by drop-casting on a hot plate. (b) The mobility distribution collected from 21 OFETs.

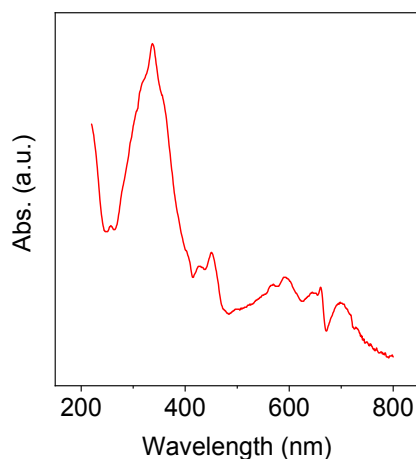


Figure S10. UV-Vis of the TIPS-pentacene uniaxial OSCMAs.

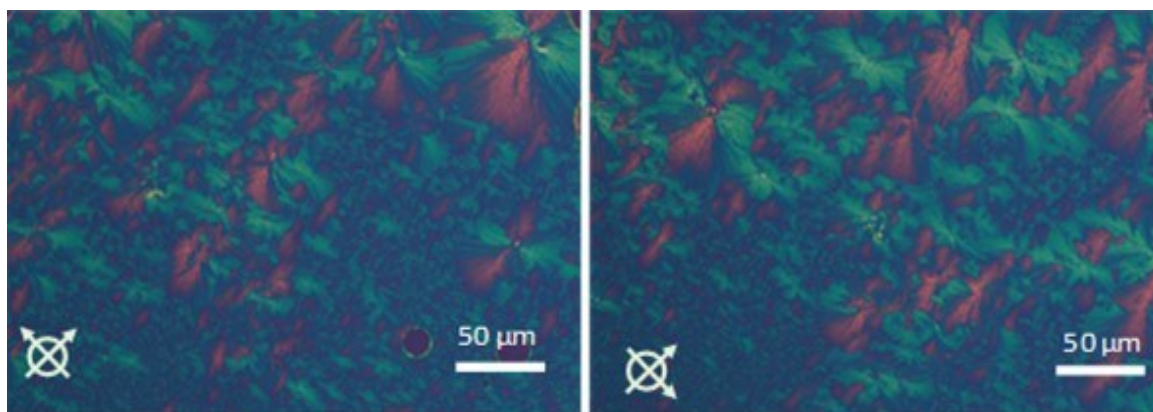


Figure S11. POM images of the drop-casting TIPS-pentacene film. When the polarization angle is changed, the brightness and the color of the film in different areas changed unevenly, indicating the polycrystalline nature of the film. Thus they showed lower performances (e.g., charge carrier mobility) compared with the OSCMAs.

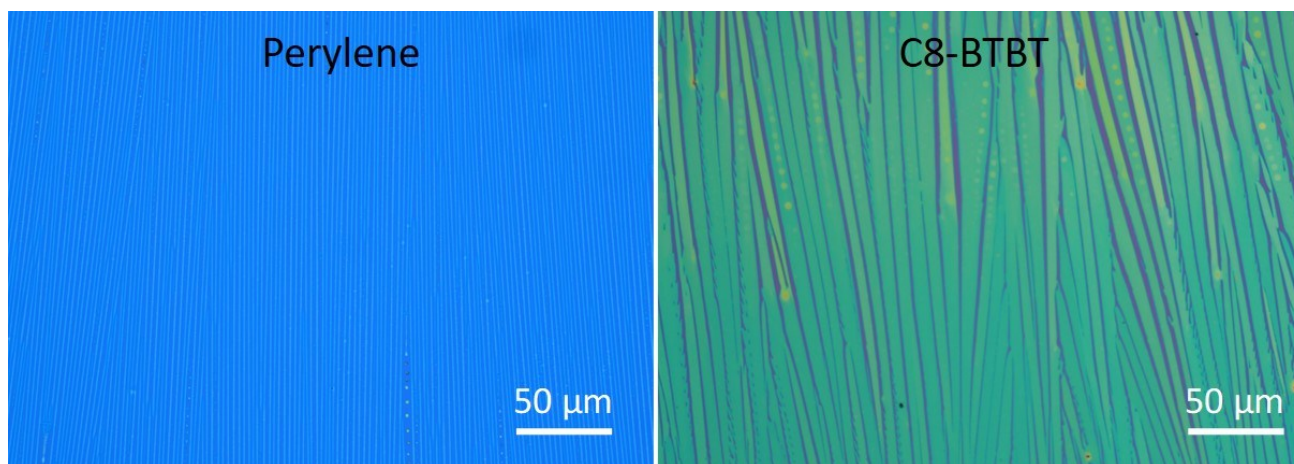


Figure S12. OM images of OSCMAs of Perylene and C8-BTBT grown by the TASA method. OSCMAs of Perylene were grown in toluene with a concentration of 3 mg/ml. the heater block was kept at 40°C. OSCMAs of C8-BTBT were grown in chlorobenzene with a concentration of 5 mg/ml. the heater block was kept at 60°C.

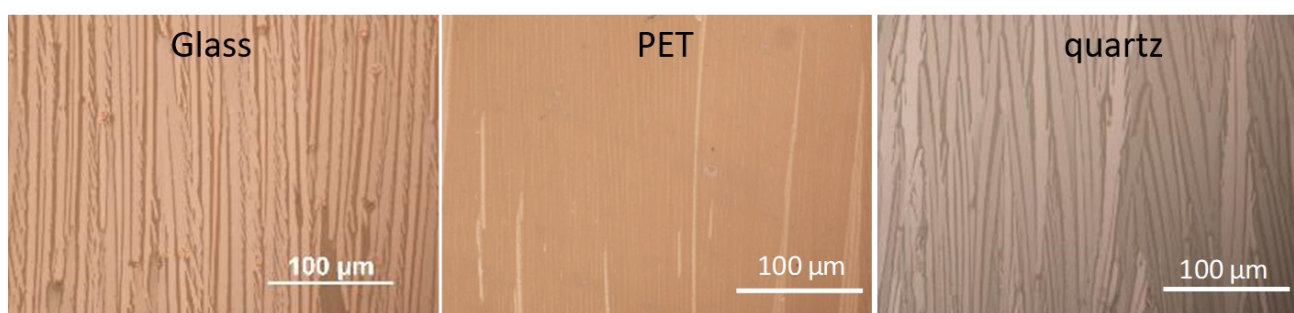


Figure S13. OM images of TIPS-pentacene grown on glass, PET and quartz. TIPS-pentacene was dissolved in toluene. The concentration was 5 mg/ml. The heater block temperature 40°C, 55°C and 60°C for glass, PET and quartz, respectively.

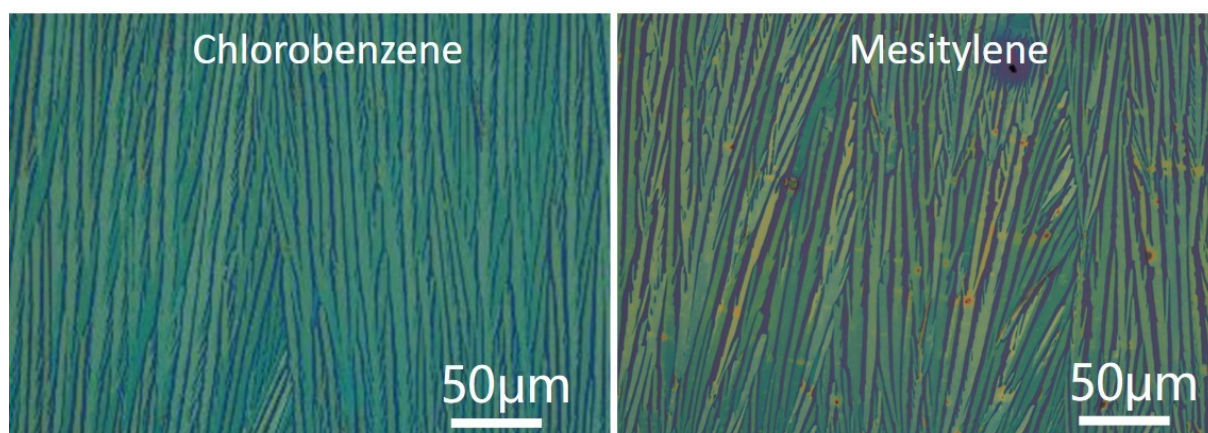


Figure S14. Typical OM images of TIPS-pentacene produced by the TASA method using chlorobenzene and mesitylene as the solvent.

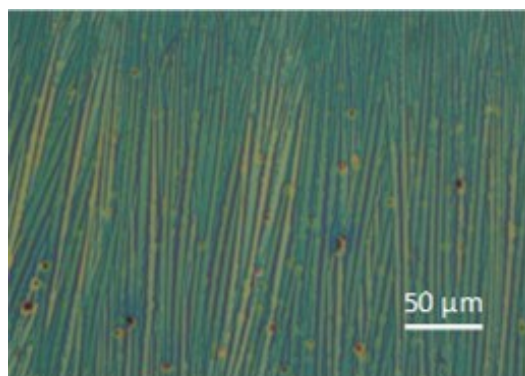


Figure S15. The OM images of TIPS-pentacene grown on OTS treated substrate.

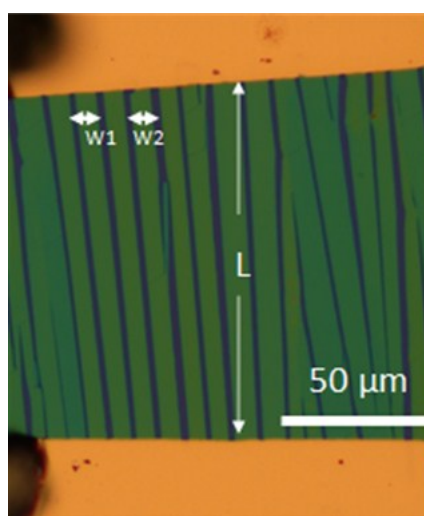


Figure S16. The channel width was the sum of the widths of the microribbons between the two electrodes.

Table S1. Comparison of figure of merit of phototransistor based on organic semiconductors.

Semiconductor	μ_{\max}	P	R	D^*	λ	Ref.
	($\text{cm}^2 \text{V}^{-1} \text{s}^{-1}$)		(AW^{-1})	(Jones)	(nm)	
BBDTE (SC*)	1.62	10^5	9.8×10^3	N/A	380	1
A-EHDTT (SC)	1.2~1.6	1.4×10^5	1.4×10^4	N/A	400	2
DNTT (TF*)	N/A	8.1×10^4	1.7×10^4	2×10^{14}	460	3
DPP-DTT/PCBM (TF)	N/A	5×10^4	350	5.7×10^{13}	810	4
C8-BTBT /polythioether (TF)	NA	1×10^5	2.5	6.3×10^{14}	350	5
BOPAnt (SC)	2.96	2×10^5	3.1×10^3	N/A	blue	6
C8BTBT:PLA (TF)	N/A	$\sim 1 \times 10^5$	393	N/A	365	7
6T (TF)	0.09	1.3×10^3	1.5~2.4	N/A	UV	8
P3HT (TF)	0.01-0.07	3.8×10^3	250	N/A	white	9
DPP-DTT/PCBM (TF)	0.14 (p) / 0.06 (n)	3×10^4	8×10^5	3×10^{12}	808	10
TFT-CN (SC)	1.36	5×10^5	9×10^4	6×10^{14}	808	11
DPA(TF)	12	8.5×10^7	1.34×10^5	1.2×10^{17}	430	12
TIPS-Pentacene (TF)	0.11(± 0.08)	1.07×10^5	2.0×10^{-2}	N/A	460	13
TIPS-Pentacene (TF)	6.3×10^{-2}	N/A	53.5×10^{-3}	N/A	white	14
TIPS-Pentacene (TF)	0.02	$10^6 \sim 10^7$	N/A	N/A	white	15
TIPS-Pentacene (SC)	2.06	1.36×10^8	845	1.98×10^{15}	365	This work

*SC: single crystal, TF: thin film

Reference

- 1 G. Zhao, J. Liu, Q. Meng, D. Ji, X. Zhang, Y. Zou, Y. Zhen, H. Dong and W. Hu, *Adv. Electron. Mater.*, 2015, **1**, 1500071.
- 2 K. H. Kim, S. Y. Bae, Y. S. Kim, J. A. Hur, M. H. Hoang, T. W. Lee, M. J. Cho, Y. Kim, M. Kim, J. I. Jin, S. J. Kim, K. Lee, S. J. Lee and D. H. Choi, *Adv. Mater.*, 2011, **23**, 3095.
- 3 Y. Chen, Y. Chu, X. Wu, W. Ou-Yang and J. Huang, *Adv. Mater.*, 2017, **29**, 1704062.
- 4 H. Xu, J. Liu, J. Zhang, G. Zhou, N. Luo and N. Zhao, *Adv. Mater.*, 2017, **29**, 1700975.
- 5 H. Peng, Y. Yan, Y. Yang, L. Zhou, W. Wu, Q. Sun, J. Zhuang, S. T. Han, C. C. Ko, Z. Xu, X. Xie, R. K. Y. Li and V. A. L. Roy, *ACS Appl. Mater. Interfaces*, 2018, **10**, 7487.

- 6 A. Li, L. Yan, M. Liu, I. Murtaza, C. He, D. Zhang, Y. He and H. Meng, *J. Mater. Chem. C*, 2017, **5**, 5304.
- 7 J. Huang, J. Du, Z. Cevher, Y. Ren, X. Wu and Y. Chu, *Adv. Funct. Mater.*, 2017, **27**, 1604163.
- 8 Y.-Y. Noh, J. Ghim, S.-J. Kang, K.-J. Baeg, D.-Y. Kim and K. Yase, *J. Appl. Phys.*, 2006, **100**, 094501.
- 9 T. Pal, M. Arif and S. I. Khondaker, *Nanotechnology*, 2010, **21**, 325201.
- 10 H. Xu, J. Li, B. H. Leung, C. C. Poon, B. S. Ong, Y. Zhang and N. Zhao, *Nanoscale*, 2013, **5**, 11850.
- 11 C. Wang, X. Ren, C. Xu, B. Fu, R. Wang, X. Zhang, R. Li, H. Li, H. Dong, Y. Zhen, S. Lei, L. Jiang and W. Hu, *Adv. Mater.*, 2018, **30**, 1706260.
- 12 D. Ji, T. Li, J. Liu, S. Amirjalayer, M. Zhong, Z.-Y. Zhang, X. Huang, Z. Wei, H. Dong, W. Hu and H. Fuchs, *Nat. Commun.*, 2019, **10**, 12.
- 13 D. Bharti, V. Raghuwanshi, I. Varun, A. K. Mahato and S. P. Tiwari, *IEEE Sens. J.*, 2017, **17**, 3689.
- 14 B. Gunduz and F. Yakuphanoglu, *Sens. Actuators. A*, 2012, **178**, 141.
- 15 Y.-H. Kim, J.-I. Han, M.-K. Han, J. E. Anthony, J. Park and S. K. Park, *Org. Electron.*, 2010, **11**, 1529.